

# Paleocene–Eocene climatic variation in western North America: Evidence from the $\delta^{18}\text{O}$ of pedogenic hematite

Huiming Bao\*

*Department of Geosciences, Princeton University, Princeton, New Jersey 08544*

Paul L. Koch<sup>†</sup>

*Department of Earth Sciences, University of California, Santa Cruz, California 95064*

Douglas Rumble III<sup>§</sup>

*Geophysical Laboratory, Carnegie Institution, Washington, D.C. 20015*

## ABSTRACT

Reconstruction of the pre-Pleistocene climate of continental interiors has been hampered by a lack of climatic proxies and limited temporal resolution. We developed a new approach based on the oxygen isotope composition ( $\delta^{18}\text{O}$ ) of hematite, which occurs as a coating on fossil vertebrates, and used this method to study climatic change across the Paleocene-Eocene boundary in the Bighorn basin, Wyoming.

Hematite coatings form in soils or shallow sediments, and therefore may be used to monitor near-surface conditions. Hematite  $\delta^{18}\text{O}$  values are measured by combining selective leaching, laser fluorination, and mass-balance calculation. These values, in conjunction with  $\delta^{18}\text{O}$  values for co-occurring carbonates, are used to assess the plausibility of published hematite-water oxygen isotope fractionation relations. Though uncertainty remains as to the appropriate fractionation, all are relatively insensitive to temperature variations. Thus, differences in hematite  $\delta^{18}\text{O}$  values most likely reflect shifts in surface-water  $\delta^{18}\text{O}$  values.

Analysis of hematites spanning the Paleocene-Eocene transition reveals a roughly 4‰ decrease in the  $\delta^{18}\text{O}$  of surface water in very early Eocene time. This episode probably reflects a cooling event (perhaps as great as 6 °C) that started 0.7 m.y. after the terminal Paleocene  $\delta^{13}\text{C}$  excursion, which corresponds to a pulse of extreme marine warming. Following the cooling, which lasted ~0.6 m.y., temperatures rebounded to values close to those for late Paleocene time. The cooling episode coincides

remarkably well with other indicators of environmental and climatic change from the basin, such as mammalian turnover events and mean annual temperatures estimated from leaf physiognomy.

## INTRODUCTION

Isotopic records from marine microfossils show a long-term warming of bottom waters and middle- to high-latitude surface waters, spanning ca. 58 to 52 Ma (Zachos et al., 1994). A brief (~150 k.y.) pulse of marine warming was superimposed on the long-term trend in latest Paleocene time, ca. 55 Ma (Kennett and Stott, 1991; Corfield and Norris, 1996). Paleocene-Eocene warming also affected continental regions (Robert and Chamley, 1991). Evidence from paleontological proxies suggests frost-free climates to 50°N in the interior of North America (Wing et al., 1991; Markwick, 1994). Physiognomic analysis of floras from Wyoming indicates an increase in mean annual temperature (MAT) from ~10 °C in late Paleocene time (Tiffanian) to ~20 °C in early Eocene time (late Wasatchian) (Wing et al., 1991). Moderate seasonality in precipitation and temperature has been inferred from paleosols and fossil floras (Bown and Kraus, 1981a; Wing and Greenwood, 1993). The key biotic events that mark the Paleocene-Eocene transition on land, in particular the first appearances of mammalian orders and species, are tightly correlated with the pulse of extreme warming in the marine record (Koch et al., 1995). Faunal turnover could reflect in situ evolution, due to forcing by climatic change, or a global expansion of taxa that had evolved slowly in low-latitude regions following climatic amelioration (Krause and Maas, 1990).

Unfortunately, the history and dynamics of equable climates in continental interiors remain poorly understood. General circulation models of Eocene climate do not easily reproduce the warm winters inferred from paleontological proxies

(Sloan, 1994; Greenwood and Wing, 1995). High-resolution data (e.g., at an ~0.1 m.y. interval) on continental climatic variations are exceedingly rare for the Paleocene-Eocene transition. Such data would be useful for evaluating atmospheric general circulation models and the stability of land climates during warm episodes in Earth history. They are essential to resolution of the impact of local versus global climate change on biotic turnover.

The marine climate record can be reconstructed using a wide range of methods. However, analysis of paleoclimatic change in the highly variable continental realm has proven more difficult. The chief methods applicable to periods prior to the Pleistocene are analyses based on pollen, leaf shapes, faunal or floral distributions, and the isotope chemistry of authigenic minerals and fossils. Studies of mineral  $\delta^{18}\text{O}$  values have been used to assess the conditions of mineral formation. The  $\delta^{18}\text{O}$  of a mineral is determined by the temperature at which it forms and the  $\delta^{18}\text{O}$  of the water from which it precipitates: the latter may be sensitive to ambient temperature in continental settings (Dansgaard, 1964). Knowledge of ancient meteoric water  $\delta^{18}\text{O}$  values would also aid understanding of vapor transport into continental interiors in the past.

Calcium carbonate and clay minerals have been the main minerals used for isotopic study of soils (Cerling and Quade, 1993; Koch et al., 1995; Amundson et al., 1996; Liu et al., 1996; Savin and Hsieh, 1998). The hydrogen and oxygen isotope compositions of iron oxides have been used to reconstruct climate on land (Yapp, 1987, 1993). Most previous studies of the  $\delta^{18}\text{O}$  of iron oxides concern either relatively recent time intervals or individual ancient sites that lack sufficient stratigraphic control to observe paleoclimatic variations in a temporal sequence. In this paper we examine the oxygen isotope composition of hematite ( $\alpha\text{-Fe}_2\text{O}_3$ ) from Paleocene-Eocene paleosols in the Bighorn basin, Wyoming, from a

\*Present address: Department of Chemistry, Mail Code 0356, University of California, San Diego, 9500 Gilman Drive, La Jolla, California 92093-0356; e-mail: hbao@cheecs2.ucsd.edu.

<sup>†</sup>E-mail: pkoch@rupture.ucsc.edu.

<sup>§</sup>E-mail: rumble@gl.ciw.edu.

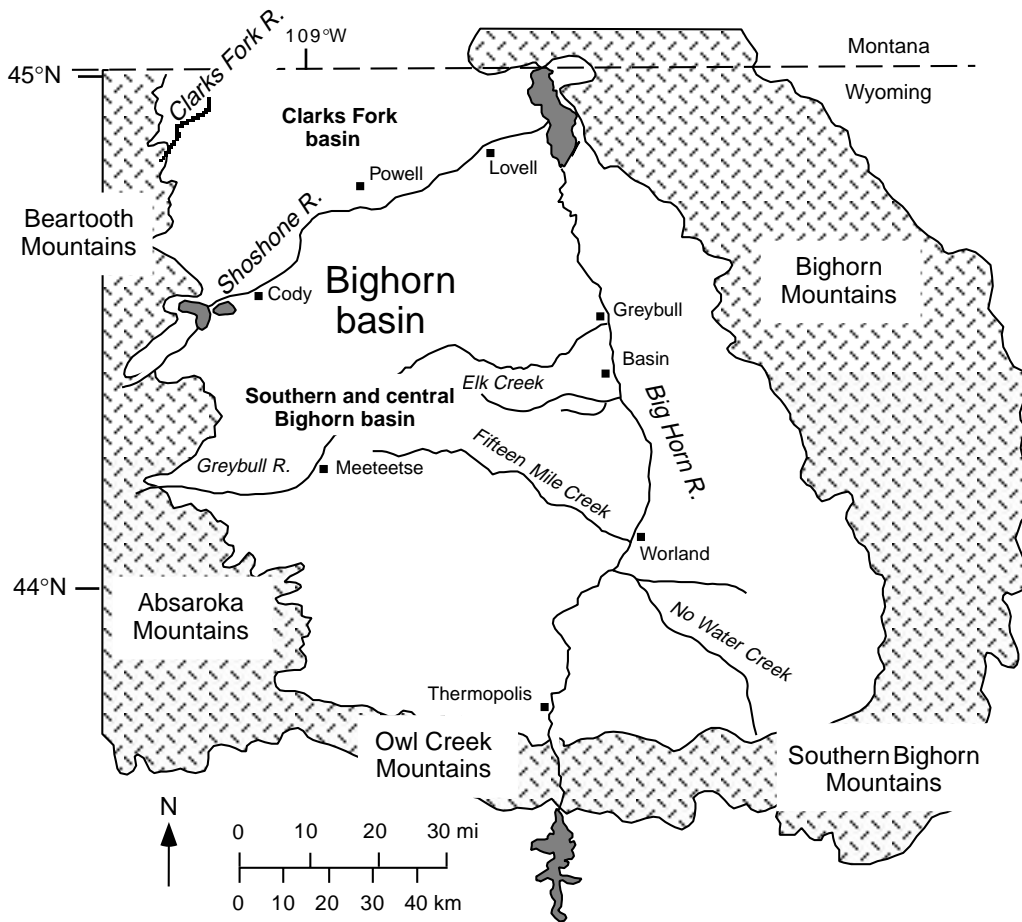


Figure 1. Map of the Bighorn basin, northwestern Wyoming. Hematite samples were from both the Clarks Fork basin and the southern and central Bighorn basin.

>3 m.y. interval (56–52.8 Ma) across the Paleocene-Eocene boundary. These data are used to document fluctuations in the  $\delta^{18}\text{O}$  of surface water across the Paleocene-Eocene boundary and their paleoclimatic implications.

#### MATERIALS AND GEOLOGIC SETTING

The Bighorn basin, located in northwestern Wyoming, is a structural and topographic basin that is surrounded by several mountain ranges uplifted during the middle and later stages of the Laramide orogeny (Fig. 1). Fossil vertebrates and plants from the Fort Union and Willwood Formations of the Bighorn basin provide the richest and most completely sampled continental record of the Paleocene-Eocene transition. Paleosols formed on hundreds of different horizons in the thick stack of flood-plain and channel deposits that accumulated in the basin from late Paleocene to early Eocene time. It has been estimated that individual paleosols formed in thousands to tens of thousands of years, on the basis of the number of paleosols, the time span of sediment accumulation, and a paleosol maturation index (Bown

and Kraus, 1993; Kraus and Bown, 1993). Soil development was interrupted by periodic flooding and crevasse-splay events.

Our samples are from two composite stratigraphic sections: the southern-central Bighorn basin section and the Clarks Fork basin section (Clarks Fork basin) in the northern Bighorn basin (Fig. 1). Faunal zonation of the southern-central Bighorn basin follows Schankler (1980), as modified by Bown et al. (1994); zonation of the Clarks Fork basin follows Gingerich (1991). Major episodes of biotic turnover across the Paleocene-Eocene boundary are similar in the southern-central Bighorn basin and Clarks Fork basin (Bown and Kraus, 1993; Bown et al., 1994; Badgley, 1989). The first episode of turnover occurred at the boundary between the Clarkforkian and the Wasatchian land mammal ages (stage Wa 0 of Gingerich, 1991), corresponding to 0 m in the southern-central Bighorn basin and 1520 m in the Clarks Fork basin (Fig. 2). The event was marked by the disappearance of 14 mammalian species and the appearance of >16 species. The second turnover corresponds to Schankler's biohorizon A, which occurs at ~200 m in the southern-central

Bighorn basin and 1750–1790 m in the Clarks Fork basin,<sup>1</sup> though its position in the Clarks Fork basin has been hampered by sampling problems (Badgley, 1989). Biohorizon A is marked by the disappearance of seven species and the appearance of eight species. The third faunal event, corresponding to a combination of Schankler's biohorizons B and C (~380–530 m in the southern-central Bighorn basin and ~2200 m in the Clarks Fork basin), was marked by the disappearance of 16 species and the appearance of 25 species (Bown and Kraus, 1993). In the southern-central Bighorn basin, biohorizon A separates Schankler's lower and upper *Haplomylus-Ectocion* range zones, and biohorizon B separates the upper *Haplomylus-Ectocion* range zone from the *Bunophorus* interval zone (Fig. 2). In the Clarks Fork basin, biohorizon A separates Wa 2 from Wa 3, and biohorizon B separates Wa 4 from Wa 5 (Gingerich, 1991).

<sup>1</sup>In the southern and central Bighorn basin, the stratigraphic position is measured relative to the base of the Willwood Formation, while in the Clarks Fork basin, the stratigraphic position is relative to the base of the Paleocene Fort Union Formation.

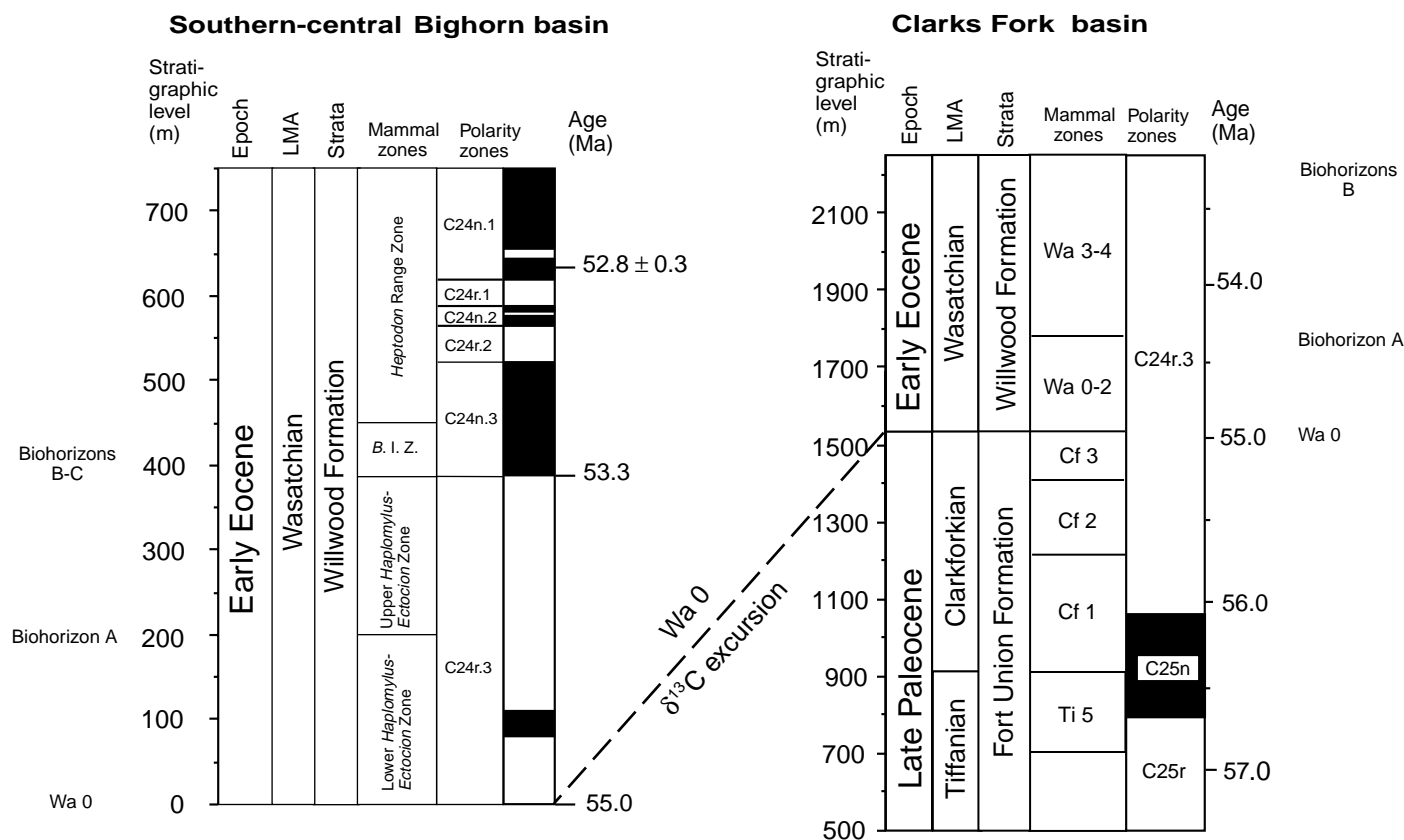


**Figure 2.** North American Land Mammal “age” (LMA), mammalian zones, and turnover events (Shankler, 1980; Badgley, 1989; Gingerich, 1991), geomagnetic polarity zones (Butler et al., 1981; Tauxe et al., 1994) (as interpreted in Wing et al., 1999), and radiometric age (Wing et al., 1991) for the Clarks Fork basin and southern-central Bighorn basin composite sections. *B.I.Z.* refers to the *Bunophorus* interval zone. The age model is described in detail in Wing et al. (1999). The model uses ages for the magnetic polarity transitions from Cande and Kent (1995), a radiometric date for a tuff in the southern-central Bighorn basin, and a calibration point determined in the McCulloughs Peak section (described in Clyde et al., 1994), assuming that the sedimentation rate within C24n.3 can be extrapolated for 70 m to calculate the age for the base of *B.I.Z.* The age for the carbon isotope excursion/Wa 0 (54.95 Ma) is determined in the Clarks Fork basin by interpolation assuming linear sedimentation between the *B.I.Z.* and the top of C25n. Wa—Wasatchian; Cf—Clarkforkian; Ti—Tiffanian.

These stratigraphic sections have been tied to the magnetic polarity time scale, providing an excellent correlation of local biotic events to global paleoclimatic events (Butler et al., 1981; Bown et al., 1994; Clyde et al., 1994; Tauxe et al., 1994). Our age model is based on the  $^{40}\text{Ar}/^{39}\text{Ar}$  date of an ash layer, an estimated age for the carbon isotope shift from the marine record, and ages for magneto-chron boundaries (Wing et al., 1999) (Fig. 2).

Highly concentrated purple-red hematite is commonly found coating fossil vertebrates. We obtained hematite samples spanning from late Clarkforkian to middle Wasatchian time from specimens collected by expeditions from Johns Hopkins University and the U.S. Geological Survey (currently housed at the Smithsonian Institution), and from collections at the Museum of Paleontology, University of Michigan, Ann Arbor, and the Peabody Museum of Yale University.

Each sample has been located in one of the composite sections for the southern-central Bighorn basin and the Clarks Fork basin (Bown et al., 1994; Gingerich et al., 1980) (Fig. 2).

Understanding the timing of hematite formation and its diagenetic history is critical to evaluating the usefulness of hematite  $\delta^{18}\text{O}$  values for paleoclimatic research. Hematite coatings are found only on vertebrate fossils, not in the soil matrix or on nodules or invertebrate fossils in paleosols. The occurrence of hematite coatings is closely associated with hydromorphic paleosols and is limited to particular horizons within these paleosols (class A gray mudstones) (Bown and Kraus, 1981a, 1981b; Bown et al., 1994). Petrographic observations, together with carbon and oxygen isotopic data from different generations of calcite, reveal that both hematite and micrite precipitated in a pedogenic environment. Clay (smectite) mineralogy and data on the geother-

mal history of the Bighorn basin (Omar et al., 1994) suggest that these paleosol deposits have not undergone burial temperatures greater than 70 °C. Given these observations, we conclude that hematite coatings formed near the Earth’s surface and therefore they provide a monitor of surface-water  $\delta^{18}\text{O}$  values for paleoclimatic research (Bao et al., 1998).

**METHODS**

We use a mass-balance approach to calculate the oxygen isotopic composition of hematite, which is intimately intergrown with silicate minerals. We leached samples drilled from hematite-rich coatings to remove highly soluble phases (which reduces potential sources of error), determined the oxygen mole fraction of hematite and silicates ( $X_{\text{hematite}}$  and  $X_{\text{silicates}}$ ) in the remaining hematite-silicate mixture by in-

ductively coupled plasma-optical emission spectrometry (ICP-OES), measured the  $\delta^{18}\text{O}$  of the hematite-silicate mixture ( $\delta^{18}\text{O}_{\text{mixture}}$ ) and the silicate residue remaining after dissolution of hematite ( $\delta^{18}\text{O}_{\text{silicates}}$ ) by laser fluorination, then calculated the  $\delta^{18}\text{O}$  of pure hematite ( $\delta^{18}\text{O}_{\text{hematite}}$ ) by mass balance.

### Chemical Pretreatment

Hematite occurring in a polymineralic mixture was collected by drilling under a microscope. Fine particles were used for analysis in order to avoid sample heterogeneity. X-ray diffraction (XRD) patterns of sample powders, including those collected after each chemical treatment, were examined. Samples were pretreated with 1M HCl for 36 hr and then 2%–3% NaOCl overnight at room temperature to remove calcite, apatite, and organic contaminants. The sample was then treated once or twice with hot (~95 °C) 5M NaOH solution. XRD and ICP analyses demonstrate that smectite and amorphous minerals are completely removed and that quartz and more resistant clays (e.g., muscovite and chlorite) are partially removed in this step. A fraction of the sample was treated with 6M HCl at 80 °C to dissolve hematite, leaving a residue of quartz and highly resistant clay minerals. XRD patterns do not show significant differences in mineral compositions between silicates in the hematite-silicate mixture after NaOH treatment and silicates in this final residue. ICP analyses indicate slightly preferential dissolution of Al-bearing minerals during the 6M HCl treatment. Fortunately, the difference is small (e.g., Si/Al ratio in mixture and in silicate residue were 6.8 and 7.8 for sample SC138, 3.8 and 5.4 for sample SC40). Thus, the contribution of silicates lost at this stage to error in the final  $\delta^{18}\text{O}$  value for the calculated hematite end member is minimal.

### ICP Analysis

The elemental composition of the sample after 5M NaOH treatment is determined by ICP-OES (Perkin Elmer 6000, Department of Geosciences, Princeton University). Fe concentration is determined by an acid-digestion method, and Si and Al concentrations are determined by the  $\text{LiBO}_2$ -fusion method. ICP analyses of six selected samples suggest that after chemical pretreatment with HCl, NaOCl, and NaOH, the concentrations of other elements such as Ca, Mn, Mg, Ti, K, and P are extremely low. Therefore, these elements are not measured in most of our samples. Each ICP-OES analysis was performed in duplicate. Precision is  $\pm 1\%$  in weight for Fe and  $\pm 2\%$ – $3\%$  in weight for Si and Al. Concentration differences between duplicates are within 2% in weight (Table 1).

TABLE 1. OXYGEN MOLE FRACTIONS (OMF) OF THE OXIDE COMPONENTS IN NaOH-TREATED HEMATITE COATINGS

Sample	O in $\text{Fe}_2\text{O}_3$ ( $\mu\text{mol}$ )	O in $\text{Al}_2\text{O}_3$ ( $\mu\text{mol}$ )	O in OH ( $\mu\text{mol}$ )*	O in $\text{SiO}_2$ ( $\mu\text{mol}$ )	OMF as hematite	X error ( $\pm$ )
<b>Clarks Fork Basin</b>						
SC171	153.65	5.07	2.25	18.75	0.855	0.000
SC92	85.25	10.28	4.57	129.30	0.372	0.007
SC127	152.25	6.44	2.86	20.95	0.834	0.005
SC90	139.84	7.38	3.28	39.97	0.734	0.012
SC90(D)	142.35	8.73	3.88	39.82	0.731	0.000
SC138	130.41	8.82	3.92	57.14	0.651	0.002
SC40	161.46	6.24	2.78	23.34	0.833	0.005
SC4	136.99	7.55	3.35	47.88	0.700	0.015
SC123	142.26	6.71	2.98	35.56	0.759	0.009
SC18	145.41	7.37	3.27	37.78	0.750	0.000
SC12	153.80	7.35	3.27	34.71	0.772	0.008
SC313	134.75	10.40	4.62	52.84	0.665	0.003
SC34	135.46	10.41	4.63	49.82	0.676	0.009
SC232	599.26	27.99	12.44	146.19	0.763	0.000
<b>Southern/central Bighorn Basin</b>						
YPM115	482.43	20.65	9.18	98.87	0.789	0.005
YPM119	633.17	25.85	11.49	99.78	0.822	0.002
YPM104	142.53	11.18	4.97	54.81	0.668	0.017
YPM290	165.01	8.72	3.88	37.94	0.766	0.005
YPM350	125.79	7.36	3.27	59.50	0.642	0.006
YPM350(D)	142.88	7.43	3.30	43.94	0.723	0.007
D1374	149.32	7.54	3.35	33.87	0.769	0.004
D1301	158.36	7.42	3.30	21.44	0.831	0.020
D1300	143.76	7.12	3.17	36.00	0.756	0.024
D1454	121.60	7.82	3.48	60.67	0.628	0.035
D1398	123.64	7.84	3.48	65.09	0.618	0.026
D1531	106.50	9.73	4.32	86.95	0.513	0.004
D1467	130.36	11.70	5.20	51.02	0.657	0.008
YPM1	229.97	17.07	7.59	108.83	0.633	0.026
YPM33	723.48	29.16	12.96	133.66	0.805	0.005

\*Calculated from oxygen mole fraction (X) as Al oxide, assuming a H/Al molar ratio of 2/3 based on the clay compositions of silicate residues (chlorite, muscovite, and sparse illite).

†Difference in OMF of hematite between duplicates divided by two.

### Laser Fluorination

Oxygen isotope analysis of sample powders was conducted by laser fluorination at the Geophysical Laboratory, Carnegie Institution, Washington, D.C. (Rumble and Hoering, 1994). Powders (1–2 mg) were loaded into a nickel holder for room-temperature, overnight,  $\text{BrF}_5$  pretreatment prior to isotopic analysis. Oxygen was generated by fluorination with a  $\text{CO}_2$  laser in a  $\text{BrF}_5$  atmosphere. Laser heating started at low power to avoid sputtering of powder. Ultimately the sample was repeatedly scanned at full power to ensure complete reaction. Evolved  $\text{O}_2$  was collected in an evacuated vessel containing a molecular sieve at  $-196$  °C, then immediately analyzed as  $\text{O}_2$  on a Finnigan MAT 252. The oxygen yields were generally 95%–102% of the calculated yield. The small oxygen deficit probably reflects moisture adsorbed during weighing (which is removed by prefluorination), and perhaps sample ejection during laser heating. Duplicate analyses were conducted for each hematite-silicate mixture, and the  $\delta^{18}\text{O}$  difference between duplicates was generally  $<0.2\%$  (29 pairs). The mean value was used for calculation of  $\delta^{18}\text{O}_{\text{hematite}}$ . Duplicate isotope analysis was not performed on silicate residues because the ~2 mg sample used in analysis came from ~20 mg of hematite-silicate mix-

ture, and thus should be thoroughly homogenized, and even a 1‰ difference in  $\delta^{18}\text{O}$  between duplicates will not affect the calculated value for  $\delta^{18}\text{O}_{\text{hematite}}$ , due to the small amount of silicates in the sample. During the course of this project (2 yr), the actual output power of the  $\text{CO}_2$  laser was consistent (~5 W). Reference samples were analyzed daily in each sample set. A magnetite reference sample (68-44C-2) gave a consistent value of  $4.1\% \pm 0.1\%$  ( $n = 21$ ), and a quartz reference (NBS-28) had a value of  $8.0\% \pm 0.15\%$  ( $n = 8$ ).

Oxygen isotope ratios (R) are expressed as  $\delta^{18}\text{O}$  values relative to V-SMOW (standard mean ocean water):

$$\delta^{18}\text{O}(\%) = \left[ \left( \frac{R_{\text{sample}}}{R_{\text{V-SMOW}}} \right) - 1 \right] \times 1000, \quad (1)$$

where  $R = {}^{18}\text{O}/{}^{16}\text{O}$ .

### Mass-Balance Calculation

The  $\delta^{18}\text{O}$  of hematite is calculated using the following mass-balance relationship:

$$\delta^{18}\text{O}_{\text{mixture}} = \delta^{18}\text{O}_{\text{hematite}} \times X_{\text{hematite}} + \delta^{18}\text{O}_{\text{silicates}} \times X_{\text{silicates}} \quad (2)$$

This approach is similar to that used by Bird et al. (1992) to determine the  $\delta^{18}\text{O}$  of modern lateritic iron oxides. Error for each estimate of  $\delta^{18}\text{O}_{\text{hematite}}$  is chiefly due to error associated with ICP analysis (i.e., the difference between the duplicate analyses of each sample). The mean error value generated by ICP analysis is  $\pm 0.4\text{‰}$  (29 pairs). In addition, the average precision associated with isotopic analysis by laser fluorination (i.e., the difference between the duplicate isotopic analyses of the same sample) is  $\pm 0.1\text{‰}$  (29 pairs). Thus, a conservative estimate for the total error associated with  $\delta^{18}\text{O}_{\text{hematite}}$  values determined by the mass-balance method ranges from 0.5‰ to 1‰.

### Additional Sources of Error

Several research groups have noted that the  $\delta^{18}\text{O}$  values from some silicates obtained by  $\text{CO}_2$  laser fluorination are systematically lower (1‰–1.5‰) than the values obtained using the conventional method of Clayton and Mayeda (1963) (Fouillac and Girard, 1996; Kirschner and Sharp, 1997). The reason for the shift has yet to be determined, but solutions to the problem have been proposed (Kirschner and Sharp, 1997; Spicuzza et al., 1998). In our experiments, the  $\delta^{18}\text{O}$  of NBS-28 is consistently 1.6‰ lower than the accepted value of 9.6‰, probably due to the low output power used (~5 W). However, the  $\delta^{18}\text{O}$  value of the reference magnetite is the same as that obtained by the conventional method. As long as the negative shift in  $\delta^{18}\text{O}$  value for the silicate residue is the same as the shift for silicates in the hematite-silicate mixture, the calculated value of  $\delta^{18}\text{O}_{\text{hematite}}$  will not be affected by the silicate problem.

To examine the effect of hematite on the fluorination of silicates, we analyzed five artificially mixed samples of NBS-28 and pure synthesized hematite with a known  $\delta^{18}\text{O}$  value. Analysis of the five samples with different proportions of NBS-28 and hematite yielded a  $\delta^{18}\text{O}$  value of 7.5‰  $\pm$  1.6‰ for NBS-28, overlapping the  $\delta^{18}\text{O}$  value for pure NBS-28 in our experiments. The large standard deviation results from the strong sensitivity of the test to weighing errors and to the ejection of quartz from mixtures during laser heating. We conclude that the presence of hematite does not conspicuously alter the negative shift in  $\delta^{18}\text{O}$  value for coexisting silicates resulting from laser fluorination. Consequently, the  $\delta^{18}\text{O}_{\text{hematite}}$  calculated from the  $\delta^{18}\text{O}$  of hematite-silicate mixture and the silicate residue should not be affected by the ongoing problem with laser fluorination of silicates.

Another potential source of error is prefluorination, which might partially react with some silicates. However, the silicate residue obtained after hot NaOH and HCl treatment is primarily a mix-

ture of quartz and minor components of muscovite and chlorite, which should be minimally affected by room temperature  $\text{BrF}_3$  treatment. Furthermore, due to the relatively low oxygen mole fraction of silicate residue in NaOH-leached samples (mean value = 0.285,  $1\sigma = 0.106$ ,  $n = 29$ ), early silicate loss would have minimal effect on the calculated value of  $\delta^{18}\text{O}_{\text{hematite}}$ .

To test the reliability of the method, we analyzed whole process duplicates (i.e., two samples from the same fossil that were collected and processed separately) on two samples: YPM350 from 290 m in the southern-central Bighorn basin and SC90 from 1455 m in the Clarks Fork basin. The consistency of  $\delta^{18}\text{O}_{\text{hematite}}$  for samples collected from the same stratigraphic level at different localities was examined by analyzing samples from two levels: D1300 and D1301 from 378 m in the southern-central Bighorn basin, and SC4 and SC123 from 1570 m in the Clarks Fork basin, which are separated by lateral distances of ~0.2 and ~13.8 km, respectively. The  $\delta^{18}\text{O}$  differences are 0.1‰ and 0.5‰ for the two whole process duplicates, and 0.8‰ and 1.2‰ for samples from the same stratigraphic levels. These errors are within the overall analytical error range for our samples.

### RESULTS

We analyzed 29 hematite samples from 25 different stratigraphic levels in both parts of the basin. Sample stratigraphic levels, estimated ages, oxygen mole fractions, and isotope results are shown in Table 2. The  $\delta^{18}\text{O}$  of hematite for both regions are combined and plotted versus estimated age (Fig. 3).

The oldest hematite sample is from 1090 m in the Clarks Fork basin. This sample has the highest  $\delta^{18}\text{O}$  value of any sample analyzed. Latest Paleocene hematites from the Clarks Fork basin have stable  $\delta^{18}\text{O}$  values of ~–12‰. In the Clarks Fork basin,  $\delta^{18}\text{O}_{\text{hematite}}$  decreases gradually by ~1‰ from the Clarkforkian-Wasatchian boundary ca. 55.0–54.4 Ma (Fig. 3). The one inconsistency between data sets from the Clarks Fork basin and the southern-central Bighorn basin occurs in this interval. Even though samples from both regions of the basin exhibit similar values from 54.6 to 54.5 Ma, at 54.9 Ma the sample YPM115 (30 m in the southern-central Bighorn basin) has a value 3‰ lower than coeval samples from the Clarks Fork basin (e.g., SC4 and SC123 from 1570 m). At present, there is no satisfactory explanation for this difference. Hematites from both regions exhibit a dramatic drop of 3‰ to 4‰ in  $\delta^{18}\text{O}$  value in very early Eocene time, from 54.5 to 54.3 Ma (Fig. 3). Low values persisted for ~0.9 m.y., from 54.3 to 53.4 Ma, followed by a quick rebound by 2‰ to 3‰ in less than 0.2 m.y., from 53.4 to 53.2 Ma.

The occurrence of this large negative shift in  $\delta^{18}\text{O}_{\text{hematite}}$  in very early Eocene time in both parts of the basin, despite differences in sedimentation rate, soil development, and tectonic influences, strongly suggests that this was an event of at least a regional scale.

### DISCUSSION

#### Evaluation of Different Hematite-Water Fractionation Relations

The ultimate goal of this study is to reconstruct the isotopic composition of surface water as a proxy for changes in local temperature and hydrology. Before attempting to convert  $\delta^{18}\text{O}_{\text{hematite}}$  values into estimated surface-water  $\delta^{18}\text{O}$  values, however, we must evaluate outstanding questions concerning oxygen isotope fractionation<sup>2</sup> between iron oxides and water. There are currently different fractionation relations for the hematite-water system in the literature, which were obtained from different approaches.

**Estimates of  $\alpha$  from Synthesis Experiments.** Controlled synthesis experiments at low pH and low rates of ferric oxide crystallization produced the following oxygen isotope fractionation relation for iron (III) oxide-water system at near surface temperatures (Yapp, 1990):

$$1000\ln\alpha = 1.63 \times 10^6/T^2 - 12.3. \quad (3)$$

Equation 3 indicates that  $\delta^{18}\text{O}_{\text{hematite}}$  should be ~6‰–9‰ more positive than formation water under surface conditions, with a temperature dependence ~–0.14‰ per °C. This is roughly 60% that of the calcite-water system, which has a fractionation relation

$$1000\ln\alpha = 2.78 \times 10^6/T^2 - 2.89 \quad (4)$$

and a temperature dependence ~–0.24‰ per °C under surface conditions (Friedman and O'Neil, 1977).

According to equation 3, and the –11.4‰ to –17.3‰ range observed for Bighorn basin hematite, we estimate that formation-water  $\delta^{18}\text{O}$  values ranged from –23.5‰ to –17.5‰ (at 25 °C) to –25.5‰ to –19.5‰ (at 10 °C). No recent soil-surface-water systems with such negative  $\delta^{18}\text{O}$  values support abundant warm-climate plants and animals, as in Paleocene-Eocene deposits from Wyoming. There are Eocene fluid-inclusion data that suggest meteoric water  $\delta^{18}\text{O}$

<sup>2</sup> $\delta^{18}\text{O}_{\text{mineral}} - \delta^{18}\text{O}_{\text{water}} \approx 1000\ln\alpha = A \times 10^6/T^2 + B$ , where T is in kelvin and A and B are empirically determined constants. The fractionation factor  $\alpha = R_{\text{mineral}}/R_{\text{water}}$ , where R is the ratio of  $^{18}\text{O}$  to  $^{16}\text{O}$  in the molecule.

TABLE 2. SAMPLE METER LEVELS, ESTIMATED AGES, ELEMENTAL COMPOSITIONS, MEASURED  $\delta^{18}\text{O}$  VALUES OF MIXTURES AND SILICATE RESIDUES, AND CALCULATED  $\delta^{18}\text{O}$  VALUES OF HEMATITE (WITH ASSOCIATED ERROR) FROM THE BIGHORN BASIN, WYOMING

Sample	Estimated age (Ma)	Stratigraphic level (m)	X <sub>hematite</sub>	X <sub>silicates</sub>	$\delta^{18}\text{O}$ <sub>mixture</sub> (‰)	$\delta^{18}\text{O}$ <sub>silicates</sub> (‰)	$\delta^{18}\text{O}$ <sub>hematite</sub> (‰)	Total error (±‰)
<b>Clarks Fork basin</b>								
SC171	55.86	1090	0.855	0.145	-7.6	14.9	-11.4	0.2
SC92	55.61	1210	0.372	0.628	4.9	15.0	-12.3	0.5
SC127	55.30	1355	0.834	0.166	-8.3	10.7	-12.0	0.4
SC90*	55.09	1455	0.734	0.266	-5.4	13.4	-12.1	0.4
SC90(D)*	55.09	1455	0.731	0.269	-5.2	13.7	-12.1	0.2
SC138	55.00	1500	0.651	0.349	-3.7	14.1	-13.3	0.2
SC40	54.92	1535	0.833	0.167	-7.8	15.6	-12.4	0.2
SC4†	54.85	1570	0.700	0.300	-4.9	14.2	-13.1	0.6
SC123†	54.85	1570	0.759	0.241	-5.7	13.6	-11.9	0.3
SC18	54.74	1620	0.750	0.250	-6.0	15.8	-13.2	0.2
SC12	54.53	1720	0.772	0.228	-6.5	16.1	-13.1	0.3
SC313	54.41	1780	0.665	0.335	-3.9	14.5	-13.2	0.2
SC34	54.26	1850	0.676	0.324	-6.2	14.6	-16.1	0.4
SC232	54.16	1895	0.763	0.238	-8.0	13.9	-14.8	0.2
<b>Southern/central Bighorn basin</b>								
YPM115	54.83	30	0.789	0.211	-9.4	14.2	-15.7	0.2
YPM119	54.54	100	0.822	0.178	-8.7	14.0	-13.6	0.2
YPM104	54.37	140	0.668	0.332	-3.9	15.1	-13.3	0.7
YPM290	54.08	210	0.766	0.235	-9.1	15.8	-16.7	0.2
YPM350§	53.75	290	0.642	0.358	-4.8	15.0	-15.8	0.3
YPM350(D)§	53.75	290	0.723	0.277	-7.8	14.4	-16.2	0.3
D1374	53.56	336	0.769	0.231	-8.8	16.0	-16.3	0.2
D1301#	53.41	378	0.831	0.169	-10.5	13.8	-15.5	0.7
D1300#	53.41	378	0.756	0.244	-8.7	14.8	-16.3	1.0
D1454	53.33	409	0.628	0.372	-3.2	16.6	-14.9	1.8
D1398	53.26	438	0.618	0.382	-2.8	14.9	-13.7	1.2
D1531	53.15	485	0.513	0.487	-0.2	15.6	-15.2	0.2
D1467	53.01	546	0.657	0.343	-4.0	16.5	-14.6	0.4
YPM1	52.95	571	0.633	0.367	-3.3	13.8	-13.2	0.5
YPM33	52.88	601	0.805	0.196	-8.6	14.0	-14.1	0.2

\*, §Whole process duplicates.

†, #Replicates from the same stratigraphic levels at different localities.

values of  $-19.1\text{‰} \pm 1.4\text{‰}$  ( $1\sigma$ ) (Seal and Rye, 1993). These data are not as negative as those inferred from hematite for Wyoming, despite the fact that these Idaho inclusions likely formed at much higher altitudes than those of Bighorn basin (Wing and Wolfe, 1993), enhancing their  $^{18}\text{O}$  depletion.

It is difficult to reconcile the extremely low meteoric  $\delta^{18}\text{O}$  values calculated for Bighorn basin hematite using equation 3 with  $\delta^{18}\text{O}$  values for coexisting micrite, bivalve aragonite, and sparry calcite. Micritic calcite is a pedogenic mineral that is intergrown with hematite, suggesting near-synchronous formation in surface deposits (Bao et al., 1998). Micrite has  $\delta^{18}\text{O}$  values ranging from 20‰ to 23‰ (V-SMOW), which imply equilibrium  $\delta^{18}\text{O}$  values for formation waters ranging from  $-8\text{‰}$  to  $-5\text{‰}$  (at 25 °C), to  $-12\text{‰}$  to  $-9\text{‰}$  (at 10 °C) using equation 4. The only temperature-formation-water  $\delta^{18}\text{O}$  combinations that jointly explain hematite and micrite  $\delta^{18}\text{O}$  values occur at unreasonably low values, below  $-20$  °C and  $-20\text{‰}$  (Fig. 4A). If micrite has been affected by diagenetic recrystallization or contamination by spar, which tends to decrease  $\delta^{18}\text{O}$  values in the Bighorn basin case (Koch et al., 1995), the field of overlap for near-synchronous formation of hematite and unaltered micrite would be even

less plausible. Evaporation or warm-season growth might cause the formation water of micrite to have a higher  $\delta^{18}\text{O}$  value than that for hematite from the same hydrologic system. Enrichments of  $\sim 10\text{‰}$ , which are required to explain the difference in formation-water  $\delta^{18}\text{O}$  value between hematite and micrite in the surface temperature range, have only been observed in extremely arid environments (Liu et al., 1996). Fossil evidence and hydromorphic features in paleosols preclude the possibility of desert conditions in Wyoming across the Paleocene-Eocene boundary. Oxygen isotope analysis of pristine, aragonitic fresh-water bivalves from the Bighorn basin (ranging in  $\delta^{18}\text{O}$  value from 17.8‰ to 22.2‰), which grow in a biologically limited range of temperatures, indicates that surface waters ranged in  $\delta^{18}\text{O}$  value between  $-14\text{‰}$  and  $-8\text{‰}$  (Koch et al., 1995), consistent with surface-water  $\delta^{18}\text{O}$  values estimated from pedogenic micrite, but not from hematite using equation 3.

Alternatively, we could assume that hematite recrystallizes postdepositionally, in equilibrium with the deep basinal fluids from which late-forming sparry calcite precipitated. These spars have  $\delta^{18}\text{O}$  values ranging from 12‰ to 14‰ (Koch et al., 1995). If we assume formation temperatures for deep basinal precipitates of 50 to

70 °C (the maximum estimate allowed based on clay mineral evidence [Bao et al., 1998]), hematite data require formation-water  $\delta^{18}\text{O}$  values 6‰–9‰ lower than those of co-occurring spar (Fig. 4A). Hematite and sparry calcite formation conditions overlap at temperatures below 30 °C, but this temperature range is low for basinal brines, assuming either modern or Eocene geothermal gradients (Omar et al., 1994). If we assume that sparry calcite and hematite formed from basinal brines at these low temperatures, we still must explain why pedogenic micrite, which also forms in this temperature range, precipitated from much more  $^{18}\text{O}$ -enriched formation waters.

Overall, it is extremely difficult to reconcile the  $\delta^{18}\text{O}$  data for our multiple mineral system with Yapp's (1990) low pH iron (III) oxide-water fractionation relation (equation 3). These discrepancies suggest that this fractionation relation may not be applicable to the Bighorn basin hematite samples. Our recent synthesis experiments obtained a slightly different fractionation relation with lower temperature dependence than that of Yapp (1990) (Bao and Koch, 1999). Although the possibility of disequilibrium fractionation in a natural hematite-water system cannot be ruled out definitely (C. Yapp, 1996, personal commun.), fractionation relations obtained from

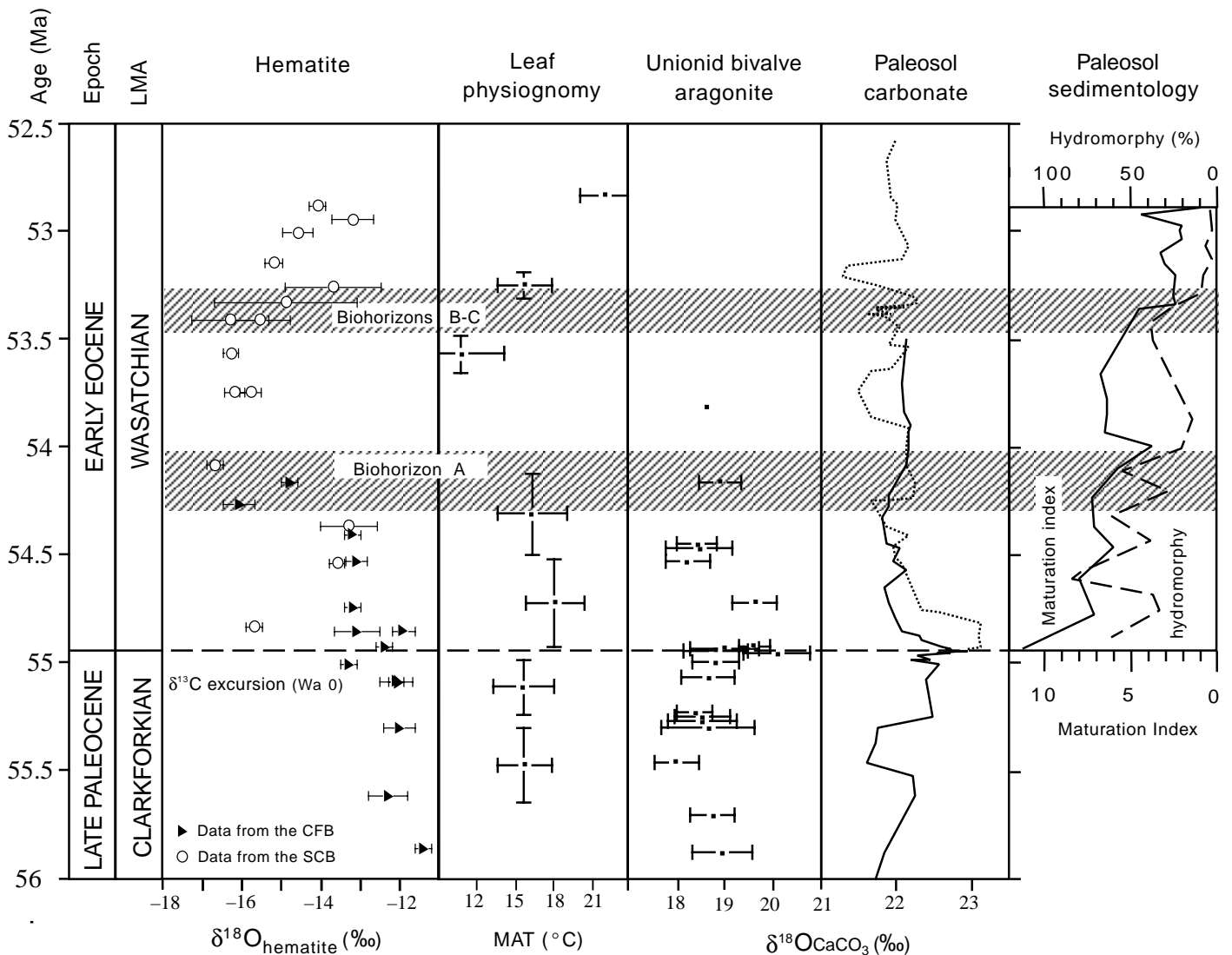


**Figure 3.** Oxygen isotope values for hematite plotted against estimated ages for Paleocene-Eocene (P-E) transition in the Bighorn basin and comparison of different paleoclimatic proxies during the P-E transition in the Bighorn basin, Wyoming. Leaf-margin analysis data are from Wing et al. (1999). Bivalve aragonite  $\delta^{18}\text{O}$  values are for the Clarks Fork basin (CFB) (data from Koch et al., 1995). Data on the  $\delta^{18}\text{O}$  of soil carbonates are from both the CFB (solid line) and the central-southern Bighorn basin (SCB) (dotted line) and are plotted as a three point running average. The plot of paleosol maturity and incidence of hydromorphy against ages are adapted from Bown and Kraus (1993). The two shaded areas are time ranges of biohorizon A and biohorizon B-C, respectively. P-E boundary is indicated by  $\delta^{13}\text{C}$  excursion (Wa 0). Error bars represent  $\pm 1\sigma$  for all data. MAT—mean annual temperature.

synthesis experiments are subject to the same problem.

**Estimates of  $\alpha$  from Semitheoretical Calculation.** Using a modified increment method, Zheng (1991) obtained the following hematite-water oxygen isotope fractionation relation for temperatures ranging from 0 to 1000 °C:

$$1000\ln\alpha = 2.69 \times 10^6/T^2 - 12.82 \times 10^3/T + 3.78. \quad (5)$$

Equation 5 yields hematite  $\delta^{18}\text{O}$  values

$\sim -6\text{‰}$  to  $-9\text{‰}$  more negative than those of formation water under surface conditions, with a temperature dependence  $\sim -0.07\text{‰}$  per °C, roughly 30% that of calcite-water system. According to Figure 4B, hematite and micrite could both have formed between 15 and 70 °C from water ranging in  $\delta^{18}\text{O}$  value from  $-8\text{‰}$  to  $0\text{‰}$ . These conditions are more plausible for both minerals than those derived using equation 3. However, estimates of the  $\delta^{18}\text{O}$  of formation water are generally higher than those suggested by fresh-water bivalve aragonite.

**Estimates of  $\alpha$  from Coexisting Minerals.**

Early work on the oxygen isotope composition of iron oxides reached a tentative conclusion that the oxygen isotope fractionation might be minimal at Earth surface temperatures (Dole and Slobod, 1940). Clayton and Epstein (1961) inferred a hematite-water fractionation relation:

$$1000\ln\alpha = 0.413 \times 10^6/T^2 - 2.56, \quad (6)$$

from hydrothermal systems with coexisting minerals such as quartz, calcite, and hematite. Equa-

tion 6 yields hematite  $\delta^{18}\text{O}$  values  $\sim 2\text{‰}$  to  $3\text{‰}$  more positive than those of formation water under surface conditions, with a temperature dependence only  $-0.04\text{‰}$  per  $^{\circ}\text{C}$ , roughly 15% that of calcite-water system. Using equation 6,  $\delta^{18}\text{O}$  values for formation water ranging from  $-13.5\text{‰}$  to  $-19.5\text{‰}$  are estimated from  $\delta^{18}\text{O}_{\text{hematite}}$ . This range slightly overlaps the lower range of water  $\delta^{18}\text{O}$  values estimated from bivalve aragonite at surface temperatures (Fig. 4B). The overlap among hematite, soil carbonate, and bivalve aragonite is much improved, however, if typical evaporative and/or seasonal effects ( $+2\text{‰}$  to  $+4\text{‰}$   $^{18}\text{O}$  enrichment) are considered for soil calcite formation relative to formation of hematite and bivalve aragonite.

In summary, isotopic data from coexisting calcite phases, together with petrographic information, suggest that the experimentally determined, low pH hematite-water fractionation relation (equation 3; Yapp, 1990) cannot explain our results from natural hematites. Although the fractionation relation estimated by semitheoretical calculation (equation 5; Zheng, 1991) provides plausible results, the match to constraining geochemistry remains poor. Clayton and Epstein's (1961) fractionation relation yields estimates for the  $\delta^{18}\text{O}$  of formation water that most closely match constraining geochemistry, as does the fractionation relation derived from the two data points from Yapp's (1987) high pH synthesis experiments (method 1). This relation need to be examined further in the laboratory and field.

Both equations 5 and 6 show a much lower temperature dependence of oxygen isotope fractionation in the hematite-water system than is observed in the calcite-water system under surface conditions, making hematite an excellent indicator of changes in the  $\delta^{18}\text{O}$  of surface water.

#### Factors Influencing the Surface-Water-Hematite Relationship

Recent studies have examined the  $\delta^{18}\text{O}$  of modern soil carbonates and their relationship to that of local mean annual precipitation (Cerling and Quade, 1993; Liu et al., 1996). The  $\delta^{18}\text{O}$  of soil water in equilibrium with soil carbonate can be from  $2\text{‰}$  to  $10\text{‰}$  higher than that of local mean annual precipitation, depending on the climate (Cerling and Quade, 1993; Liu et al., 1996; Hsieh et al., 1998). This phenomenon results from evaporative  $^{18}\text{O}$  enrichment of soil water and/or preferential formation of soil carbonate in the summer.

There are a few studies of the  $\delta^{18}\text{O}$  values of modern soil iron oxides and local meteoric water (Bird et al., 1992; Girard et al., 1997; Yapp, 1997). Different types of pedogenic iron oxides may show different relationships to local mete-

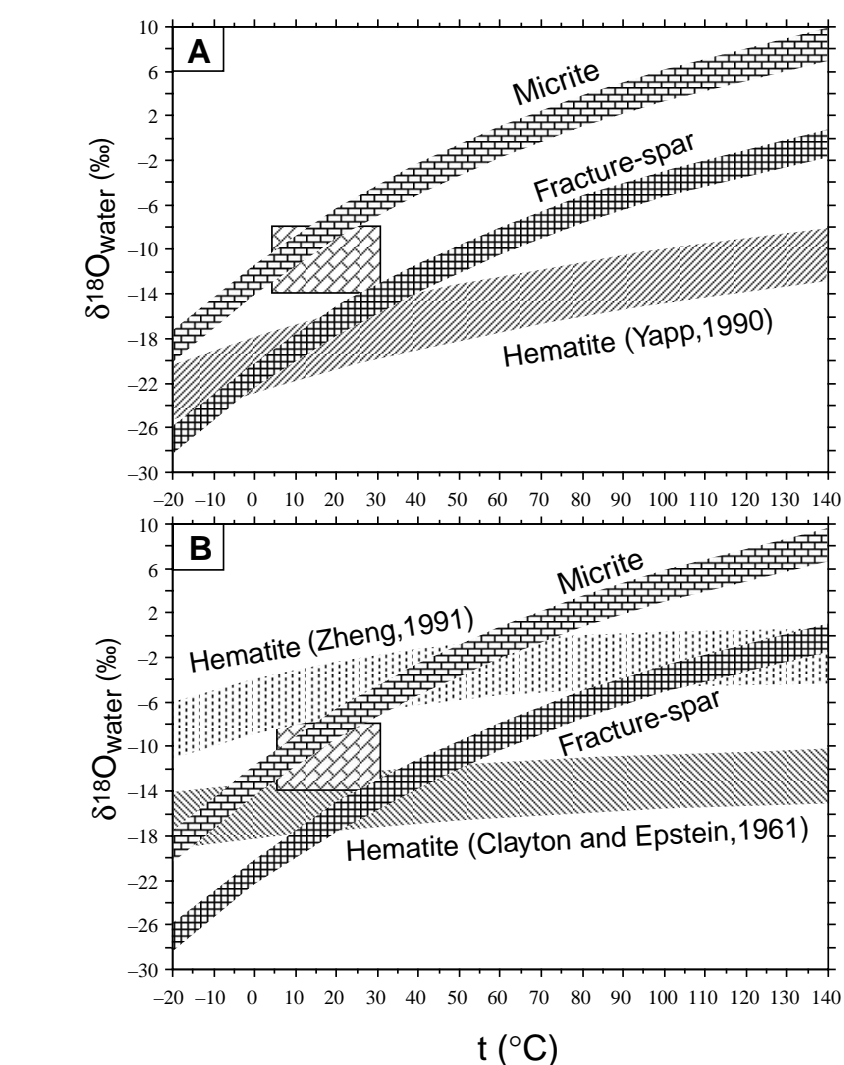


**Figure 4.** Combinations of temperature and formation-water  $\delta^{18}\text{O}$  values that can jointly explain the observed  $\delta^{18}\text{O}$  data for micrite, sparry calcite, and hematite in the Bighorn basin. The rectangle on the left is the area representing possible formation conditions for bivalve aragonite (data from Koch et al., 1995). (A) Hematite trend calculated using the fractionation relation of Yapp (1990). (B) Hematite trend calculated using the fractionation relations of Zheng (1991) and Clayton and Epstein (1961).

oric water, owing to differences in formation conditions and pathways. For example, goethites from lateritic regolith may be  $^{18}\text{O}$  enriched due to evaporation (Bird et al., 1992). Petrographic and pedogenic observations suggest that Bighorn basin hematite coatings likely record the  $\delta^{18}\text{O}$  value for soil or shallow ground water, perhaps integrated over a time interval as great or slightly greater than that of pedogenesis (Bao et al., 1998). However, in the absence of an investigation of similar ferric oxide coatings in modern soils, the exact relation between the  $\delta^{18}\text{O}$  of meteoric water and that of hematite formation water remains undetermined. Although this information is important for estimates of the absolute

value of paleoclimatic parameters, it is not as critical when reconstructing relative changes in these parameters through time, as long as hematite coatings from different stratigraphic levels equilibrated with the same type of surface water. For our paleoclimatic interpretations, we will assume that all hematite coatings formed under similar geochemical conditions in which the relation between the  $\delta^{18}\text{O}$  of formation water and the  $\delta^{18}\text{O}$  of mean meteoric water was constant.

#### Early Eocene Cooling?

In temperate and polar regions, the mean  $\delta^{18}\text{O}$  of meteoric water exhibits a strong, positive cor-

relation with mean annual temperature (MAT) (Dansgaard, 1964; Rozanski et al., 1993). This is a spatial relationship, however. A reliable temporal  $\delta^{18}\text{O}/\text{MAT}$  relationship has to be used in order to estimate the MAT change through time in one particular location. A study of global water isotope geochemistry during the last glacial maximum (LGM) using a general circulation model suggests that the spatial  $\delta^{18}\text{O}/\text{MAT}$  relationships for the present-day and LGM climates are very similar. The study also suggests that the temporal  $\delta^{18}\text{O}/\text{MAT}$  relationship is on average similar to the present-day spatial relationship over wide areas (Jouzel et al., 1994), although a calculation including tropical cooling and seawater  $\delta^{18}\text{O}$  increase during the LGM may reduce the slope of the temporal  $\delta^{18}\text{O}/\text{MAT}$  relationship (Boyle, 1997). If the negative shift in the  $\delta^{18}\text{O}$  value of surface water in the Bighorn basin in early Eocene time was due entirely to regional or global cooling, the relative decrease in MAT can be very roughly estimated using the modern spatial  $\delta^{18}\text{O}/\text{MAT}$  relationship, which has a slope of  $\sim 0.6\text{‰}–0.7\text{‰}/^\circ\text{C}$  for middle- to high-latitude continental sites data (Rozanski et al., 1993). Therefore, the  $\sim 4\text{‰}$  drop in the  $\delta^{18}\text{O}$  value of surface water, reconstructed from  $\delta^{18}\text{O}_{\text{hematite}}$ , implies a drop in MAT ranging from  $\sim 5.5$  to  $6.5$   $^\circ\text{C}$ . The estimated MAT decrease is much larger if the relationship from Boyle (1997) (slope =  $0.37\text{‰}/^\circ\text{C}$ ) or Beyerle et al. (1998) (slope =  $0.49\text{‰}/^\circ\text{C}$ ) is used.

However, the presence of high mountains between the source of moisture and the basin may lead to greater  $^{18}\text{O}$  depletion of water without large changes in local MAT, both through input of meltwater runoff and through the arrival of vapor masses that are extremely  $^{18}\text{O}$  depleted due to the loss of moisture during passage over mountain ranges. Major structural events in the Bighorn basin during early Cenozoic time include the uplift of the northern Bighorn, Pryor, and Beartooth Mountains from Late Cretaceous through Eocene time, the uplift of the southern Bighorn Mountains and Owl Creek Mountains in late Paleocene time, and the thrusting of these mountains to the south in middle early Eocene time (Bown, 1980). In this generally active tectonic background, no dramatic events have been closely associated in time with biohorizons A and B–C. Second-order changes in the rate of basin subsidence that are probably related to mountain uplift are inferred from the changes in paleosol maturity at these levels (Fig. 3). A decrease in paleosol maturity, as seen at biohorizons A and B–C, might signal a relative increase in mountain uplift rate, which would increase the sediment load to the basin and decrease the time for soil formation between sedimentation events on the flood plain. However, if an abrupt rise of adjacent

mountains caused a  $\delta^{18}\text{O}$  decrease in surface water, then uplift can only explain the decrease in values at biohorizon A. The rise in  $\delta^{18}\text{O}$  values at biohorizons B–C would imply a decrease in the height of adjacent mountains. However, paleosol maturity shows a sharp decrease at this level, suggesting further increase in mountain uplift rate. It seems unlikely, therefore, that tectonic events alone can explain the early Eocene rise and fall in hematite  $\delta^{18}\text{O}$  values in the Bighorn basin.

In addition, shifts in the source of moisture from the Gulf of Mexico to the North Pacific may contribute to changes in the  $\delta^{18}\text{O}$  of precipitation in continental North America without positive correlation with changes in MAT (Amundson et al., 1996). Given our lack of knowledge of the strength of the prevailing westerlies and the northward extension of monsoonal flow in Paleocene–Eocene time in North America, as well as modeling results that suggest quite different patterns of atmospheric circulation from today (Sloan, 1994), the most conservative approach is to assume that a general relationship similar to the current global  $\delta^{18}\text{O}/\text{MAT}$  curve dominates in this mid-latitude, mid-continental region. Although change in vapor source cannot be ruled out, we believe that regional cooling is the most likely explanation for the early Eocene drop in surface-water  $\delta^{18}\text{O}$  values.

**Comparison to Floral Data.** It has long been recognized that the Paleocene–Eocene transition was a time of global warming. Thus, the cooling in very early Eocene time implied by the drop in  $\delta^{18}\text{O}_{\text{hematite}}$  was unexpected. An initial indication of early Eocene cooling from studies of fossil plant diversity and leaf shape was attributed to a paucity of plant fossils from this interval, rather than to actual cooling (Wing et al., 1991). However, recent analysis of expanded plant collections supports a cooling episode in the Bighorn basin during earliest Eocene time (Wing et al., 1999). The timing and magnitude of the change in MAT derived from  $\delta^{18}\text{O}_{\text{hematite}}$  are generally similar to those from leaf-margin analysis (Fig. 3). Nevertheless, these independent proxies for MAT exhibit several differences. For example, leaf-margin analysis indicates a slight increase in MAT ( $\sim 2$   $^\circ\text{C}$ ) ca. 54.7 Ma, whereas the  $\delta^{18}\text{O}_{\text{hematite}}$  suggests a decrease in MAT. In addition, leaf-margin analysis suggests that the highest MAT occurred ca. 52.8 Ma, when the  $\delta^{18}\text{O}_{\text{hematite}}$  suggests MATs less than those of late Paleocene time. We note, however, that we lack hematite data from most of the interval that is yielding high leaf-margin MAT estimates.

The  $\sim 4\text{‰}$  drop in surface-water  $\delta^{18}\text{O}$  occurs at a time when leaf-margin analysis indicates a  $6$   $^\circ\text{C}$  drop in MAT. Coupling these independent proxies, we obtain a temporal  $\delta^{18}\text{O}/\text{MAT}$  slope of  $\sim 0.67$   $\text{‰}/^\circ\text{C}$ , very close to that of the present-day spatial

$\delta^{18}\text{O}/\text{MAT}$  relationship in this region. These data provide the first evidence that the model-simulated results of the temporal  $\delta^{18}\text{O}/\text{MAT}$  relationship, based on LGM/present-day temperature change and global water isotope geochemistry, may be applicable under a very different climatic regime in the distant past.

**Comparison to Carbonate  $\delta^{18}\text{O}$  Values.** Aragonite from fresh-water unionid bivalves, soil carbonates, and biogenic phosphates provide independent monitors of changes in surface-water  $\delta^{18}\text{O}$  values (Koch et al., 1995; Fricke et al., 1998). The average  $\delta^{18}\text{O}$  of bivalve aragonite from the Clarks Fork basin is essentially invariant from late Clarkforkian time to biohorizon A, except for a clear excursion to higher values from the Wa 0 horizons at the Clarkforkian–Wasatchian boundary (Fig. 3). The  $\delta^{18}\text{O}$  values of soil carbonates from Wa 0 beds are  $>1\text{‰}$  higher than the background of late Clarkforkian–early Wasatchian soil carbonates. The  $\delta^{18}\text{O}_{\text{hematite}}$  fails to show the positive anomaly at Wa 0 seen in soil carbonates and bivalves solely because we lack hematite coatings from this brief interval. Few bivalves have been recovered from the stratigraphic interval with low  $\delta^{18}\text{O}_{\text{hematite}}$ ; however, those that occur in the interval do not have values lower than typical late Clarkforkian or early Wasatchian bivalves. Several levels within this interval in the southern-central Bighorn basin have soil carbonates with  $\delta^{18}\text{O}$  values  $\sim 0.8\text{‰}$  lower than typical background values, whereas data from the Clarks Fork basin do not decrease at all (Fig. 3). If the  $\sim 4\text{‰}$  drop in  $\delta^{18}\text{O}_{\text{hematite}}$  (and presumably surface-water  $\delta^{18}\text{O}$ ) is associated with an  $\sim 6$   $^\circ\text{C}$  drop in MAT (as suggested by leaf-margin analysis), then the  $\delta^{18}\text{O}$  of calcite should drop by  $\sim 2.5\text{‰}$  ( $\sim 4\text{‰}$  due to the shift in water  $\delta^{18}\text{O}$  and  $\sim 1.5\text{‰}$  due to the temperature dependence of calcite-water fractionation [equation 4]). Thus, the magnitude of the decrease of carbonate  $\delta^{18}\text{O}$  in early Eocene time does not match that suggested by hematite data for the MAT change. Although carbonate data suggest a warmer MAT at the Paleocene–Eocene boundary and a cooler MAT in very early Eocene time, which is consistent with the hematite data, the carbonate  $\delta^{18}\text{O}$  data are more variable and poorly correlated with the temporal variation of hematite  $\delta^{18}\text{O}$ . This failure may relate (1) to diagenetically induced heterogeneity in the soil carbonate record and (2) to changes in the evaporative water loss from soils, which can strongly influence soil carbonate  $\delta^{18}\text{O}$  values.

**Climate and Faunal Turnover.** The large negative shift in the  $\delta^{18}\text{O}$  of surface water in the Bighorn basin began  $\sim 0.7$  m.y. after the  $\delta^{13}\text{C}$  excursion and short-term warming that mark the beginning of the Wasatchian at Wa 0 (Fig. 3). It is interesting that the interval with low  $\delta^{18}\text{O}_{\text{hematite}}$

corresponds to the upper *Haplomylus-Ectocion* zone (Schankler, 1980, 1981), which is bracketed by two major mammalian turnover events in earliest Eocene time: biohorizon A at the start of event, and biohorizons B-C at the end (Fig. 3). Schankler (1981) noted that the upper *Haplomylus-Ectocion* zone was characterized by the temporary disappearance of taxa that occurred in preceding and later zones, and he suggested that these disappearances might reflect climatically driven, temporary migration of taxa out of the basin. Our data provide strong support for this conjecture.

**Comparison with Marine Record.** The  $\delta^{13}\text{C}$  excursion in the Bighorn basin (Koch et al., 1995) correlates precisely with the large marine excursion in terminal Paleocene time. If the cooling event in early Eocene time is global, a similar episode may be present in marine records ~0.7 m.y. after the  $\delta^{13}\text{C}$  excursion. At present, a few high-resolution marine  $\delta^{18}\text{O}$  records show a similar cooling episode in this general time interval, but the precise timing of these episodes relative to the Bighorn basin record is difficult to constrain, and the data are noisy (Corfield and Norris, 1996). A study of this cooling episode on land and in the ocean will improve our understanding of the links between oceans and continental interiors under a warm climate regime.

## CONCLUSIONS

The oxygen isotope composition of hematite found on the surface of vertebrate fossils provides a new source of information on continental paleoclimates. Despite uncertainties in hematite-water fractionation, hematite can be an excellent monitor of the change of the surface-water  $\delta^{18}\text{O}$ , because the fractionation of oxygen isotopes between hematite and water is relatively independent of temperature. Resolving the discrepancies between different fractionation factors for the hematite-water system is essential for further application of this proxy to paleoclimatic reconstruction.

Changes in surface-water  $\delta^{18}\text{O}$  during the Paleocene-Eocene transition in the Bighorn basin have been derived from variations in hematite  $\delta^{18}\text{O}$ . An ~4% drop in the  $\delta^{18}\text{O}$  of surface water in very early Eocene time is best explained by a regional or global climatic cooling event, corresponding to an ~6 °C drop in MAT. The change corresponds to faunal and floral turnover and sedimentologic events in the Bighorn basin. This cooling episode in generally warm early Eocene time was largely unexpected, and it points to the need for high-resolution data to define the spatial and temporal distribution of climatic events on land, and to integrate this growing record of continental climate variation with the marine record.

## ACKNOWLEDGMENTS

This project is supported by National Science Foundation grant EAR-9627953. We thank Tom Bown for bringing the hematite coatings on fossils in the Bighorn basin to our attention. We are grateful for the generous contribution of fossils from collections at the Johns Hopkins University and U.S. Geological Society (housed at Smithsonian Museum), the Museum of Paleontology, the University of Michigan, Ann Arbor, the Peabody Museum of Yale University, and the Museum of Paleontology at the University of California. We thank Scott Wing for access to data in press on plant physiognomy. We especially thank Pat Holroyd, Gregg Gunnell, and Mary Ann Turner for their assistance in searching museum collections, and Maria Borcsik for assistance in ICP analysis. This work benefited greatly from discussions with Jerry Bigham, Will Clyde, Marilyn Fogel, Philip Gingerich, Mary Kraus, Johannes Müller, Dan Schrag, Udo Schwertmann, Scott Wing, and reviews by Crayton Yapp, Ethan Grossman, and Samuel Savin.

## REFERENCES CITED

- Amundson, R., Chadwick, O., Kendall, C., Wang, Y., and DeNiro, M., 1996, Isotopic evidence for shifts in atmospheric circulation patterns during the late Quaternary in mid-North America: *Geology*, v. 24, p. 23–26.
- Badgley, C. E., 1989, A statistical assessment of last appearances in the fossil record of Eocene Mammals, in Bown, T. M., and Rose, K. M., eds., Dawn of the age of mammals in the northern part of the Rocky Mountain interior, North America: Geological Society of America Special Paper 243, p. 153–168.
- Bao, H., and Koch, P. L., 1999, Oxygen isotope fractionation in ferric oxide-water systems: Low temperature synthesis. *Geochimica et Cosmochimica Acta*, v. 63, p. 599–613.
- Bao, H., Koch, P. L., and Hepple, R. P., 1998, Hematite and calcite coatings on fossil vertebrates: *Journal of Sedimentary Research*, ser. A, v. 65, p. 727–738.
- Beyerle, U., Purtschert, R., Aeschbach-Hertig, W., Imboden, D. M., Loosli, H. H., Wüeller, R., and Kipfer, R., 1998, Climate and groundwater recharge during the last glaciation in an ice-covered region: *Science*, v. 282, p. 731–734.
- Bird, M. I., Longstaffe, F. J., Fyfe, W. S., and Bildgen, P., 1992, Oxygen-isotope systematics in a multiphase weathering system in Haiti: *Geochimica et Cosmochimica Acta*, v. 56, p. 2831–2838.
- Bown, T. M., 1980, Summary of latest Cretaceous and Cenozoic sedimentary, tectonic, and erosional events, Bighorn Basin, Wyoming, in Gingerich, P. D., ed., Early Cenozoic paleontology and stratigraphy of the Bighorn Basin, Wyoming: University of Michigan Papers on Paleontology 24, p. 25–32.
- Bown, T. M., and Kraus, M. J., 1981a, Lower Eocene alluvial paleosols (Willwood Formation, northwestern Wyoming, USA) and their significance for paleoecology, paleoclimatology, and basin analysis: *Palaeogeography, Palaeoclimatology, Palaeoecology*, v. 34, p. 1–30.
- Bown, T. M., and Kraus, M. J., 1981b, Vertebrate fossil-bearing paleosol units (Willwood Formation, Lower Eocene, northwestern Wyoming, U.S.A.): Implications for taphonomy, biostratigraphy, and assemblage analysis: *Palaeogeography, Palaeoclimatology, Palaeoecology*, v. 34, p. 31–56.
- Bown, T. M., and Kraus, M. J., 1993, Time-stratigraphic reconstruction and integration of paleopedologic, sedimentologic, and biotic events (Willwood Formation, lower Eocene, northwest Wyoming, USA): *Palaios*, v. 8, p. 68–80.
- Bown, T. M., Rose, K. D., Simons, E. L., and Wing, S. L., 1994, Distribution and stratigraphic correlation of upper Paleocene and lower Eocene fossil mammal and plant localities of the Fort Union, Willwood, and Tatman Formations, southern Bighorn Basin, Wyoming: U. S. Geological Survey Professional Paper 1540, 103 p.
- Boyle, E. A., 1997, Cool tropical temperatures shift the global  $\delta^{18}\text{O}$ -T relationship: An explanation for the ice core  $\delta^{18}\text{O}$ -borehole thermometry conflict?: *Geophysical Research Letters*, v. 24, p. 273–276.
- Butler, R. F., Gingerich, P. D., and Lindsay, E. H., 1981, Magnetic polarity stratigraphy and biostratigraphy of Paleocene and Eocene continental deposits, Clarks Fork Basin, Wyoming: *Journal of Geology*, v. 89, p. 299–316.
- Cande, S. C., and Kent, D. V., 1995, Revised calibration of the geomagnetic timescale for the Late Cretaceous and Cenozoic: *Journal of Geophysical Research*, ser. B, v. 100, p. 6093–6095.
- Cerling, T. E., and Quade, J., 1993, Stable carbon and oxygen isotopes in soil carbonate, in Swart, P. K., Lohmann, K. C., McKenzie, J., and Savin, S., eds., Climate change in continental isotopic records: American Geophysical Union Geophysical Monograph 78, p. 217–231.
- Clayton, R. N., and Epstein, S., 1961, The use of oxygen isotopes in high-temperature geological thermometry: *Journal of Geology*, v. 69, p. 447–452.
- Clayton, R. N., and Mayeda, T. K., 1963, The use of bromine pentafluoride in the extraction of oxygen from oxides and silicates for isotopic analysis: *Geochimica et Cosmochimica Acta*, v. 27, p. 43–52.
- Clyde, W. C., Stamatakos, J., and Gingerich, P. D., 1994, Chronology of the Wasatchian Land-Mammal Age (early Eocene): Magnetostratigraphic results from the McCullough Peaks section, northern Bighorn Basin, Wyoming: *Journal of Geology*, v. 102, p. 367–377.
- Corfield, R. M., and Norris, R. D., 1996, Deep water circulation in the Paleocene ocean, in Knox, R. W. O. B., Corfield, R. M., and Dunay, R. E., eds., Correlation of the early Paleogene in northwest Europe: Geological Society [London] Special Publication 101, p. 443–456.
- Dansgaard, W., 1964, Stable isotopes in precipitation: *Tellus*, v. 16, p. 436–468.
- Dole, M., and Slobod, R. L., 1940, Isotopic composition of oxygen in carbonate rocks and iron oxide ores: *Journal of American Chemical Society*, v. 62, p. 471–479.
- Fouillac, A. M., and Girard, J.-P., 1996, Laser oxygen isotope analysis of silicate/oxide grain separates: Evidence for a grain size effect?: *Chemical Geology*, v. 130, p. 31–54.
- Fricke, H. C., Clyde, W. C., O'Neil, J. R., and Gingerich, P. D., 1998, Evidence for rapid climate change in North America during the latest Paleocene thermal maximum: Oxygen isotope compositions of biogenic phosphate from the Bighorn Basin (Wyoming): *Earth and Planetary Science Letters*, v. 160, p. 193–208.
- Friedman, I., and O'Neil, J. R., 1977, Compilation of stable isotope fractionation factors of geochemical interest: U.S. Geological Survey Professional Paper 440-kk, 12 p.
- Gingerich, P. D., 1991, Systematics and evolution of early Eocene *Perissodactyla* (Mammalian) in the Clarks Fork Basin, Wyoming: University of Michigan Contributions from the Museum of Paleontology 28, p. 181–213.
- Gingerich, P. D., Rose, K. D., and Krause, D. W., 1980, Early Cenozoic mammalian faunas of the Clark's Fork Basin-Polecat Bench area, northwestern Wyoming, in Gingerich, P. D., ed., Early Cenozoic paleontology and stratigraphy of the Bighorn Basin, Wyoming: University of Michigan Papers on Paleontology 24, p. 24–51.
- Girard, J.-P., Razaanadranoroa, D., and Freyssinet, P., 1997, Laser oxygen isotope analysis of weathering goethite from the lateritic profile of Yaou, French Guiana: Paleoweathering and paleoclimatic implications: *Applied Geochemistry*, v. 12, p. 163–174.
- Greenwood, D. R., and Wing, S. L., 1995, Eocene continental climates and latitudinal temperature gradients: *Geology*, v. 23, p. 1044–1048.
- Hsieh, J. C. C., Chadwick, O. A., Kelly, E. F., and Savin, S. M., 1998, Oxygen isotopic composition of soil water; quantifying evaporation and transpiration: *Geoderma*, v. 82, p. 269–293.
- Jouzel, J., Koster, R. D., Suozzo, R. J., and Russell, G. L., 1994, Stable water isotope behavior during the last glacial maximum: A general circulation model analysis: *Journal of*

- Geophysical Research, v. 99, p. 25791–25801.
- Kennett, J. P., and Stott, L. D., 1991, Abrupt deep-sea warming, palaeoceanographic changes and benthic extinctions at the end of the Palaeocene: *Nature*, v. 353, p. 225–229.
- Kirschner, D. L., and Sharp, Z. D., 1997, Oxygen isotope analysis of fine-grained minerals and rocks using the laser-extraction technique: *Chemical Geology*, v. 137, p. 109–115.
- Koch, P. L., Zachos, J. C., and Dettmann, D. L., 1995, Stable isotope stratigraphy and paleoclimatology of the Paleogene Bighorn Basin (Wyoming, U.S.A.): *Palaeogeography, Palaeoclimatology, Palaeoecology*, v. 115, p. 61–89.
- Kraus, M. J., and Bown, T. M., 1993, Short-term sediment accumulation rates determined from Eocene alluvial paleosols: *Geology*, v. 21, p. 743–746.
- Krause, D. W., and Maas, M. C., 1990, The biogeographic origins of late Paleocene–early Eocene mammalian immigrants to the Western Interior of North America, *in* Bown, T. M., and Rose, K. D., eds., *Dawn of the age of mammals in the northern part of the Rocky Mountain interior*: Geological Society of America Special Paper 243, p. 71–105.
- Liu, B., Phillips, F. M., and Campbell, A. R., 1996, Stable carbon and oxygen isotopes of pedogenic carbonates, Ajo Mountains, southern Arizona; implications for paleoenvironmental change: *Palaeogeography, Palaeoclimatology, Palaeoecology*, v. 124, p. 233–246.
- Markwick, P., 1994, “Equability,” continentality, and Tertiary “climate”: The crocodylian perspective: *Geology*, v. 22, p. 613–616.
- Omar, G. I., Lutz, T. M., and Giegengack, R., 1994, Apatite fission-track evidence for Laramide and post-Laramide uplift and anomalous thermal regime at the Beartooth overthrust, Montana-Wyoming: *Geological Society of America Bulletin*, v. 106, p. 74–85.
- Robert, C., and Chamley, H., 1991, Development of early Eocene warm climates, as inferred from clay mineral variations in oceanic sediments: *Palaeogeography, Palaeoclimatology, Palaeoecology* (Global and Planetary Change Section), v. 89, p. 315–331.
- Rozanski, K., Araguas-Araguas, L., and Gonfiantini, R., 1993, Isotopic patterns in modern global precipitation, *in* Swart, P. K., Lohmann, K. C., McKenzie, J., and Savin, S., eds., *Climate change in continental isotopic records*: American Geophysical Union Geophysical Monograph 78, p. 1–36.
- Rumble, D., III, and Hoering, T., 1994, Analysis of oxygen and sulfur isotope ratios in oxide and sulfide minerals by spot heating with a carbon dioxide laser in a fluorine atmosphere: *Accounts of Chemical Research*, v. 27, p. 237–241.
- Savin, S. M., and Hsieh, J. C. C., 1998, The hydrogen and oxygen isotope geochemistry of pedogenic clay minerals; principles and theoretical background: *Geoderma*, v. 82, p. 227–253.
- Schankler, D. M., 1980, Faunal zonation of the Willwood Formation in the central Bighorn Basin, Wyoming: University of Michigan Papers on Paleontology 24, p. 99–114.
- Schankler, D. M., 1981, Local extinction and ecological re-entry of early Eocene mammals: *Nature*, v. 293, p. 135–138.
- Seal, R. R., II, and Rye, R. O., 1993, Stable isotope study of fluid inclusions in fluorite from Idaho: Implications for continental climates during the Eocene: *Geology*, v. 21, p. 219–222.
- Sloan, L. C., 1994, Equable climates during the Eocene: Significance of regional paleogeography for North American climate: *Geology*, v. 22, p. 881–884.
- Spicuzza, M. J., Valley, J. W., Kohn, M. J., Girard, J. P., and Fouillac, A. M., 1998, The rapid heating, defocused beam technique: A CO<sub>2</sub>-laser-based method for highly precise and accurate determination of  $\delta^{18}\text{O}$  values of quartz: *Chemical Geology*, v. 144, p. 195–203.
- Tauxe, L., Gee, J., Gallet, Y., Pick, T., and Bown, T., 1994, Magnetostratigraphy of the Willwood Formation, Bighorn Basin, Wyoming: New constraints on the location of Paleocene/Eocene boundary: *Earth and Planetary Science Letters*, v. 125, p. 159–172.
- Wing, S. L., and Greenwood, D. R., 1993, Fossils and fossil climate: The case for equable continental interiors in the Eocene, *in* Allen, J. R. L., Hoskins, B. J., Sellwood, B. W., and Spicer, R. A., eds., *Palaeoclimates and their modeling with special reference to the Mesozoic Era*: Royal Society of London Philosophical Transactions, Biological Sciences, ser. B, v. 341, p. 243–252.
- Wing, S. L., and Wolfe, J. A., 1993, Stable isotope study of fluid inclusions in fluorite from Idaho: Implications for continental climate during the Eocene: *Comment and Reply: Geology*, v. 21, p. 1051–1052.
- Wing, S. L., Bown, T. M., and Obradovich, J. D., 1991, Early Eocene biotic and climatic change in interior western North America: *Geology*, v. 19, p. 1189–1192.
- Wing, S. L., Bao, H., and Koch, P. L., 1999, An early Eocene cool period? Evidence for continental cooling during the warmest part of the Cenozoic, *in* Huber, B. T., MacCleod, K., and Wing, S. L., eds., *Warm climates in Earth history*: Cambridge, Cambridge University Press (in press).
- Yapp, C. J., 1987, Oxygen and hydrogen isotope variations among goethites (a-FeOOH) and the determination of paleotemperatures: *Geochimica et Cosmochimica Acta*, v. 51, p. 355–364.
- Yapp, C. J., 1990, Oxygen isotopes in iron (III) oxides: 1, mineral-water fractionation factors: *Chemical Geology*, v. 85, p. 329–335.
- Yapp, C. J., 1993, The stable isotope geochemistry of low temperature Fe(III) and Al “oxides” with implications for continental paleoclimates, *in* Swart, P. K., Lohmann, K. C., McKenzie, J., and Savin, S., eds., *Climate change in continental isotopic records*: American Geophysical Union Geophysical Monograph 78, p. 285–294.
- Yapp, C. J., 1997, An assessment of isotopic equilibrium of goethites from a bog iron deposit and a lateritic regolith: *Chemical Geology*, v. 135, p. 159–171.
- Zachos, J. C., Stott, L. D., and Lohmann, K. C., 1994, Evolution of early Cenozoic marine temperatures: *Paleoceanography*, v. 9, p. 353–387.
- Zheng, Y-F., 1991, Calculation of oxygen isotope fractionation in metal oxides: *Geochimica et Cosmochimica Acta*, v. 55, p. 2299–2307.

MANUSCRIPT RECEIVED BY THE SOCIETY MARCH 23, 1998  
 REVISED MANUSCRIPT RECEIVED NOVEMBER 19, 1998  
 MANUSCRIPT ACCEPTED DECEMBER 2, 1998